Pear, W.S., Nolan, G.P., Scott, M.L., Baltimore, D., 1993. Production of high-titer helper-free retroviruses by transient transfection. Proc. Natl. Acad. Sci. USA 90, 8392–8396.

Pennisi, D., Bowles, J., Nagy, A., Muscat, G., Koopman, P., 2000. Mice null for Sox18 are viable and display a mild coat defect. Mol. Cell. Biol. 20, 9331–9336.

Schepers, G., Wilson, M., Wilhelm, D., Koopman, P., 2003. SOX8 is expressed during testis differentiation in mice and synergizes with SF1 to activate the Amh promoter in vitro. J. Biol. Chem. 278, 28101–28108.

Schwartz, S., Zhang, Z., Frazer, K.A., Smit, A., Riemer, C., Bouck, J., et al., 2000. PipMakerA web server for aligning two genomic DNA sequences. Genome Res. 10, 577–586.

Shen, W.H., Moore, C.C., Ikeda, Y., Parker, K.L., Ingraham, H.A., 1994. Nuclear receptor steroidogenic factor 1 regulates the mullerian inhibiting substance gene: a link to the sex determination cascade. Cell 77, 651–661.

Smith, C.A., Smith, M.J., Sinclair, A.H., 1999a. Gene expression during gonadogenesis in the chicken embryo. Gene 234, 395–402.

Smith, C.A., Smith, M.J., Sinclair, A.H., 1999b. Expression of chicken steroidogenic factor-1 during gonadal sex differentiation. Gen. Comp. Endocrinol. 113, 187–196.

Smits, P., Li, P., Mandel, J., Zhang, Z., Deng, J.M., Behringer, R.R., de Crombrugghe, B., Lefebvre, V., 2001. The transcription factors L-sox5 and sox6 are essential for cartilage formation. Dev. Cell 1, 277–290.

Stolt, C.C., Lommes, P., Sock, E., Chaboissier, M.C., Schedl, A., Wegner, M., 2003. The sox9 transcription factor determines glial fate choice in the developing spinal cord. Genes Dev. 17, 1677–1689.

Takada, S., DiNapoli, L., Capel, B., Koopman, P., 2004. Sox8 is expressed at similar levels in gonads of both sexes during the sex determining period in turtles. Dev. Dyn. 231, 387–395.

Takada, S., Mano, H., Koopman, P., 2005. Regulation of Amh during sex determination in chickens: sox gene expression in male and female gonads. Cell. Mol. Life Sci. 62, 2140–2146.

Takada, S., Ota, J., Kansaku, N., Yamashita, H., Izumi, T., Ishikawa, M., et al., 2006. Nucleotide sequence and embryonic expression of quail and duck sox9 genes. Gen. Comp. Endocrinol. 145, 208–213.

Watanabe, K., Clarke, T.R., Lane, A.H., Wang, X., Donahoe, P.K., 2000. Endogenous expression of Mullerian inhibiting substance in early postnatal rat sertoli cells requires multiple steroidogenic factor-1 and GATA-4-binding sites. Proc. Natl Acad. Sci. USA 97, 1624–1629.

Western, P.S., Harry, J.L., Graves, J.A., Sinclair, A.H., 1999. Temperature-dependent sex determination in the American alligator: AMH precedes SOX9 expression. Dev. Dyn. 216, 411–419.

Xu, Q., Wilkinson, D., 1998. In situ hybridisation of mRNA with hapten labelled probes. In: Wilkinson, D. (Ed.), In Situ Hybridisation: A Practical Approach, second ed. Oxford University Press, Oxford, pp. 87–106.

Zacchei, A.M., 1961. The embryonal development of the Japanese quail (*Coturnix coturnix japonica* T. and S.). Arch. Ital. Anat. Embriol. 66, 36–62.

Available online at www.sciencedirect.com
SCIENCE DIRECT®
General and Comparative Endocrinology 145 (2006) 208–213
GENERAL AND COMPARATIVE ENDOCRINOLOGY
www.elsevier.com/locate/ygcen

Communication in Genomics and Proteomics

Nucleotide sequence and embryonic expression of quail and duck *Sox9* genes

Shuji Takada [a,*], Jun Ota [a,b], Norio Kansaku [c], Hideji Yamashita [d], Tokukazu Izumi [e], Madoka Ishikawa [a], Tomoaki Wada [a], Ruri Kaneda [a], Young Lim Choi [a], Koji Koinuma [a], Shin-ichiro Fujiwara [a], Hirotaka Aoki [a], Hiroyuki Kisanuki [a], Yoshihiro Yamashita [a], Hiroyuki Mano [a,b]

[a] *Division of Functional Genomics, Jichi Medical School, 3311-1 Yakushiji, Kawachigun, Tochigi 329-0498, Japan*
[b] *CREST, Japan Science and Technology Agency, Saitama 332-0012, Japan*
[c] *Laboratory of Animal Genetics and Breeding, Azabu University, Fuchinobe, Sagamihara, Kanagawa 229-8501, Japan*
[d] *Laboratory of Genome Exploration and Informatics, Department of Bioscience, Kyushu Tokai University, Kawayo, Aso-gun, Kumamoto 869-1404, Japan*
[e] *Laboratory of Animal Reproduction, Department of Bioproduction Science, Faculty of Bioresources and Environmental Science, Ishikawa Prefectural University, Nonoichi-machi, Ishikawa 921-8836, Japan*

Received 21 February 2005; revised 17 August 2005; accepted 22 August 2005
Available online 7 October 2005

Abstract

Sox9 is a member of the *Sry*-type HMG-box (Sox) gene family. It encodes a transcription factor and is thought to be important for sexual differentiation in chicken. In the present study we have isolated *Sox9* cDNAs from quail and duck, and examined the expression patterns of the corresponding genes in early embryonic gonads by whole-mount in situ hybridization. We developed a polymerase chain reaction-based protocol to identify the sex of quail and duck embryos before its morphological manifestation. *Sox9* expression was first detected on days 5 and 7 in the gonads of male quail and duck embryos, respectively, and was not apparent in female gonads at these stages. These expression patterns are similar to that of chicken *Sox9*. Our results thus suggest that the expression of quail and duck *Sox9* is associated with testis differentiation.

Keywords: *Sox9*; Quail; Duck; Sexing; Sex determination

1. Introduction

In mammals, the heterogametic pairing of sex chromosomes (XY) results in male development, whereas males are homogametic (ZZ) and females are heterogametic (ZW) in birds. It remains unclear whether avian sex is determined by Z chromosome gene dosage, by a master female-determining gene (or genes) on the W chromosome, or by a combination of both processes (Clinton, 1998). However W chromosome dose not seem to have a decisive role, since administration of an aromatase inhibitor to genetically female embryos before sex-determining period caused about half of treated chickens develop testes (Elbrecht and Smith, 1992). It seems likely that the in vivo exposure of estrogen at an early stage of embryonic development plays a crucial role in differentiation of an ovary in chicken. In contrast, the importance of estrogens for gonadal sex differentiation in birds is not seen in mammals. Although the systems for sex determination and differentiation differ between mammals and birds, several genes that are associated with sex determination or differentiation in mammals are expressed in similar patterns in chicken and mouse gonads, suggestive of some degree of similarity between the molecular mechanisms of sexual differentiation in these two species.

* Corresponding author. Fax: +81 285 44 7322.
E-mail address: stakada@jichi.ac.jp (S. Takada).

0016-6480/$ - see front matter © 2005 Elsevier Inc. All rights reserved.
doi:10.1016/j.ygcen.2005.08.009

One such gene is *Sry-type high mobility group-box containing gene 9* (*Sox9*). *Sox9* and the related gene *Sry*, which is located on the Y chromosome, are sex determination genes in mice (Koopman et al., 1991; Vidal et al., 2001). However, *Sox9* is not thought to contribute to sex determination in chicken, given that it is expressed predominantly in developing testis only after establishment of the sexually dimorphic expression pattern of *anti-Müllerian hormone* (*Amh*), a gene associated with sexual differentiation (Oréal et al., 1998; Smith et al., 1999; Takada et al., 2005). It is instead likely that *Sox9* plays a role in sexual differentiation in chicken.

Elucidation of the molecular mechanisms of sex determination and differentiation in birds will require the identification of additional genes that are essential for these processes as well as comparative analyses of gene expression patterns and mechanisms of action between birds and other vertebrates. We have now characterized the expression patterns of *Sox9* in quail and duck embryos during the early stages of gonadal differentiation before the appearance of morphological sex differences. To distinguish the sexes at these early stages, we devised an easy and accurate sexing method based on the polymerase chain reaction (PCR).

2. Methods

2.1. Animals

Fertilized Japanese quail (*Coturnix coturnix japonica*) and domestic duck (*Anas platyrhynchos*) eggs were obtained from a local supplier (Saitama Experimental Animal Supply, Saitama, Japan) and were maintained at 18 °C until transfer to an incubator at 37.8 °C. Staging of quail embryos was confirmed at dissection according to Zacchei (1961). Staging of duck embryos was compared at dissection with chicken stages (Hamburger and Hamilton, 1951). The entire urogenital ridge of each embryo was explanted for whole-mount in situ hybridization.

2.2. PCR-based sexing

A hind limb was removed from an embryo to isolate genomic DNA for PCR-based sexing as described (Clinton et al., 2001), with minor modifications. In brief, tissue was soaked in 100 μl of digestion buffer [10 mM Tris–HCl (pH 8.0), 1 mM EDTA, 1% SDS, and proteinase K (10 μg/ml)] and incubated at 50 °C for 1 h. After phenol–chloroform extraction, 80 μl sample was diluted to 400 μl with water, and 1 μl of the diluted material was subjected to PCR. The PCR protocol comprised denaturation for 4.5 min at 95 °C followed by 40 cycles of incubation at 95 °C for 30 s and 56 °C for 30 s. The reaction was performed in a final volume of 25 μl containing 10 mM Tris–HCl (pH 8.3), 50 mM KCl, 1.5 mM $MgCl_2$, 0.001% gelatin, 0.2 mM deoxynucleoside triphosphates, 0.13 μM 18S primers (Clinton et al., 2001), 0.4 μM *Wpkci* primers, and 0.5 U of AmpliTaq Gold DNA polymerase (Applied Biosystems, Foster City, CA). The primers qWpkciF (5′-TTGGGCATTTGAAGATT GTC-3′) and qWpkciR (5′-GTCTGAAGGGTCTGA GGGT-3′) were used for sexing of quail embryos, whereas dWpkciF (5′-CTTCTTGGGCGTTTCGTG-3′) and dWpkciR (5′-G TCTGAAGGGCCCGAGGGT-3′) were used for sexing of duck embryos. PCR products together with molecular size standards (50-bp DNA ladder; Invitrogen, Carlsbad, CA) were fractionated by electrophoresis on a 4% agarose gel.

2.3. Cloning and sequencing of quail and duck Sox9 cDNAs

Partial genomic fragments of quail and duck *Sox9* were amplified by PCR in a final volume of 25 μl containing 1× NH_4 buffer (Bioline, London, UK), 0.2 mM deoxynucleoside triphosphates, 0.4 μM primers, and 0.5 U of Biotaq DNA polymerase (Bioline). The PCR protocol comprised denaturation at 95 °C for 4.5 min followed by 40 cycles of incubation at 95 °C for 30 s and 62 °C for 30 s. The primers used were qdSox9F (5′-ATGAATCTCCTAGACCCCTT C-3′) and qdSox9R (5′-GGSACCAGSGTCCAGTCGTA-3′). The PCR products were ligated into the pT7-Adv vector (Clontech, Palo Alto, CA) and sequenced by Operon Biotechnologies (Tokyo, Japan).

Quail and duck *Sox9* cDNAs were generated by 5′ and 3′ RACE. Total RNA was purified from male quail (day 7) and duck (day 8) embryonic gonads with the use of an RNeasy Mini kit (Qiagen, Valencia, CA) and was converted to double-stranded cDNA with the use of a SMART PCR cDNA Synthesis kit (Clontech). RACE was performed in a solution containing 1× NH_4 buffer (Bioline), 0.2 mM deoxynucleoside triphosphates, 0.4 μM primers, 1.8 M betaine, and 0.5 U of Biotaq DNA polymerase. The PCR protocol comprised denaturation at 95 °C for 4.5 min followed by 40 cycles of incubation at 95 °C for 30 s, 65 °C for 30 s, and 72 °C for 3 min. Betaine was included to facilitate the amplification of GC-rich target fragments (Henke et al., 1997). Primers used for the quail and duck 3′ RACE were 5′ PCR Primer IIA (Clontech) and uniSox9F1 (5′-CA GCCCCACCATGTCGGATGACTCCGC-3′), those for the quail 5′ RACE were 5′ PCR Primer IIA and uniSox9R1 (5′-TCCTTCTTCAGGTCCGGGTCGCC-3′), and those for the duck 5′ RACE were 5′ PCR Primer IIA and dSox9R6 (5′-TTGGCTCACCGCCTCTCGGATG-3′). RACE products were ligated into the pGEM-T easy vector (Promega, Madison, WI) for nucleotide sequencing. At least three independent clones were sequenced for each RACE reaction.

The complete coding sequences of quail and duck *Sox9* cDNAs were amplified by RT-PCR as for RACE with the exception that PCR was performed for 4.5 min at 95 °C followed by 40 cycles of incubation at 95 °C for 30 s, 56 °C for 30 s, and 72 °C for 2 min, and that the primers used for *qSox9* cDNA were qSox95′UTRF (5′-CTGGAGGCTCCATC TCTCCCTG-3′) and qSox93′UTRR (5′-TTTATTT GTCTT CACGTGGCT-3′) and those for *dSox9* cDNA were dSox95′UTRF (5′-CCCCCTCCGCCACTTTCTCG-3′) and

dSox93'UTRR (5'-ATGGCTTTTAGGGTCTG GTGAG-3'). RT-PCR products were ligated into pGEM-T easy.

2.4. Whole-mount in situ hybridization

Whole-mount in situ hybridization was performed as described (Xu and Wilkinson, 1998) with the maleic acid buffer method. Digoxigenin-labeled RNA probes were synthesized by in vitro transcription of cDNAs obtained by *Bam*HI digestion of 3' RACE clones of *qSox9* and *dSox9*. The probes corresponded to nucleotides 391–568 of *qSox9* cDNA (Accession No. AY904048) and nucleotides 194–371 of *dSox9* cDNA (Accession No. AY904046).

3. Results and discussion

3.1. Sexing of quail and duck embryos

To distinguish between female and male early embryos of quail or duck before the appearance of morphological sexual differences, we developed an assay based on the absence (males) or presence (females) of *Wpkci* (also known as *Asw*), which is located on the W chromosome (Hori et al., 2000; O'Neill et al., 2000). This gene was detected by PCR performed in a single tube with *Wpkci*-specific primers and, as a positive control, primers specific for the gene for 18S rRNA. Female quails are expected to generate two distinct PCR products of 101 and 256 bp for quail *Wpkci* (*qWpkci*) and the 18S rRNA gene, respectively, whereas males are expected to generate only the latter product (Fig. 1A). Female ducks are expected to yield two bands of 104 and 256 bp for duck *Wpkci* (*dWpkci*) and the 18S rRNA gene, respectively, whereas males should again generate only the latter band (Fig. 1B). The accuracy of this PCR-based sexing method was confirmed by the amplification of genomic DNA from adult birds of each species. In all cases, the results of PCR-based sexing were identical to those obtained by morphological examination (data not shown).

3.2. Cloning and sequence analysis of quail and duck Sox9 genes

To isolate *Sox9* cDNAs for quail and duck, we used the 5' and 3' rapid amplification of cDNA end (RACE) techniques (Frohman et al., 1988) with RNA purified from the gonads of male quail or duck embryos on days 7 and 8, respectively, given that *Sox9* would be expected to be expressed in the developing testis if it functions in male sexual differentiation. To design the 3' RACE primer, we amplified partial genomic fragments of quail and duck *Sox9* by PCR with a primer set based on conserved cDNA sequences for the 5' untranslated region (UTR) and the high mobility group (HMG)-box region of *Sox9* of chicken (*Gallus gallus*, U12533), American alligator (*Alligator mississippiensis*, AF106572), red-eared slider turtle (*Trachemys scripta*) (Spotila et al., 1998), mouse (*Mus musculus*, AF421878), and rainbow trout (*Oncorhynchus mykiss*, AB006448). These primers yielded 266- and 269-bp products from the quail and duck genomes, respectively (data not shown), and these products were then subjected to nucleotide sequencing.

The 3' RACE reaction was then performed with gonadal cDNA from quail or duck males and a primer based on the sequence of the conserved PCR products. The nucleotide sequences of the resulting amplicons were determined and used to design the primers for 5' RACE. The nucleotide sequences thus obtained by 5' and 3' RACE were assembled.

To confirm that the sequences determined by 5' and 3' RACE were derived from the same transcripts, we attempted to amplify cDNAs containing the entire coding regions by reverse transcription (RT) and PCR with primers localized in the 5' and 3' UTRs. A 1.6-kb cDNA was amplified from quail RNA and a 1.5-kb cDNA from duck RNA. Nucleotide sequencing of these amplified fragments confirmed that the 5' and 3' RACE sequences were linked in tandem in quail and in duck, demonstrating that the assembled sequences correspond to single transcripts.

The deduced amino acid sequences of the proteins encoded by the quail and duck cDNAs revealed that the 79-residue *Sry*-type HMG-boxes of the two proteins were identical to each other and differed by only one amino acid from that of chicken Sox9 (Fig. 2). The overall sequence identities of the three proteins were 94.3, 85.5, and 94.3% between quail and chicken, duck and chicken, and quail and duck, respectively. Given that the NH_2- and COOH-termini of the deduced amino acid sequences of the quail and duck proteins were highly conserved compared with

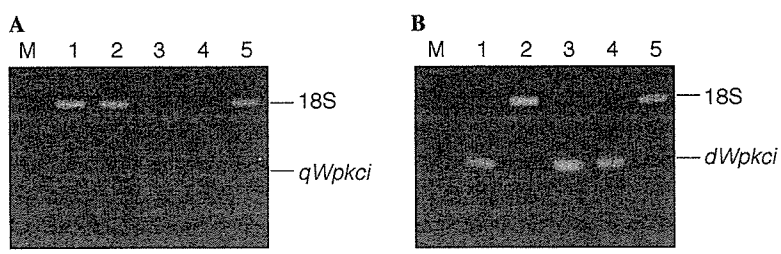

Fig. 1. PCR-based sexing of quail and duck embryos. Sexing of five embryos each of quail (A) and duck (B) was performed. Quail embryos in lanes 1, 2, and 5 are males; those in lanes 3 and 4 are females. Duck embryos in lanes 2 and 5 are males; those in lanes 1, 3, and 4 are females. The positions of PCR products corresponding to the 18S rRNA gene and *Wpkci* are indicated. Lanes M contain DNA size markers (50-bp ladder).

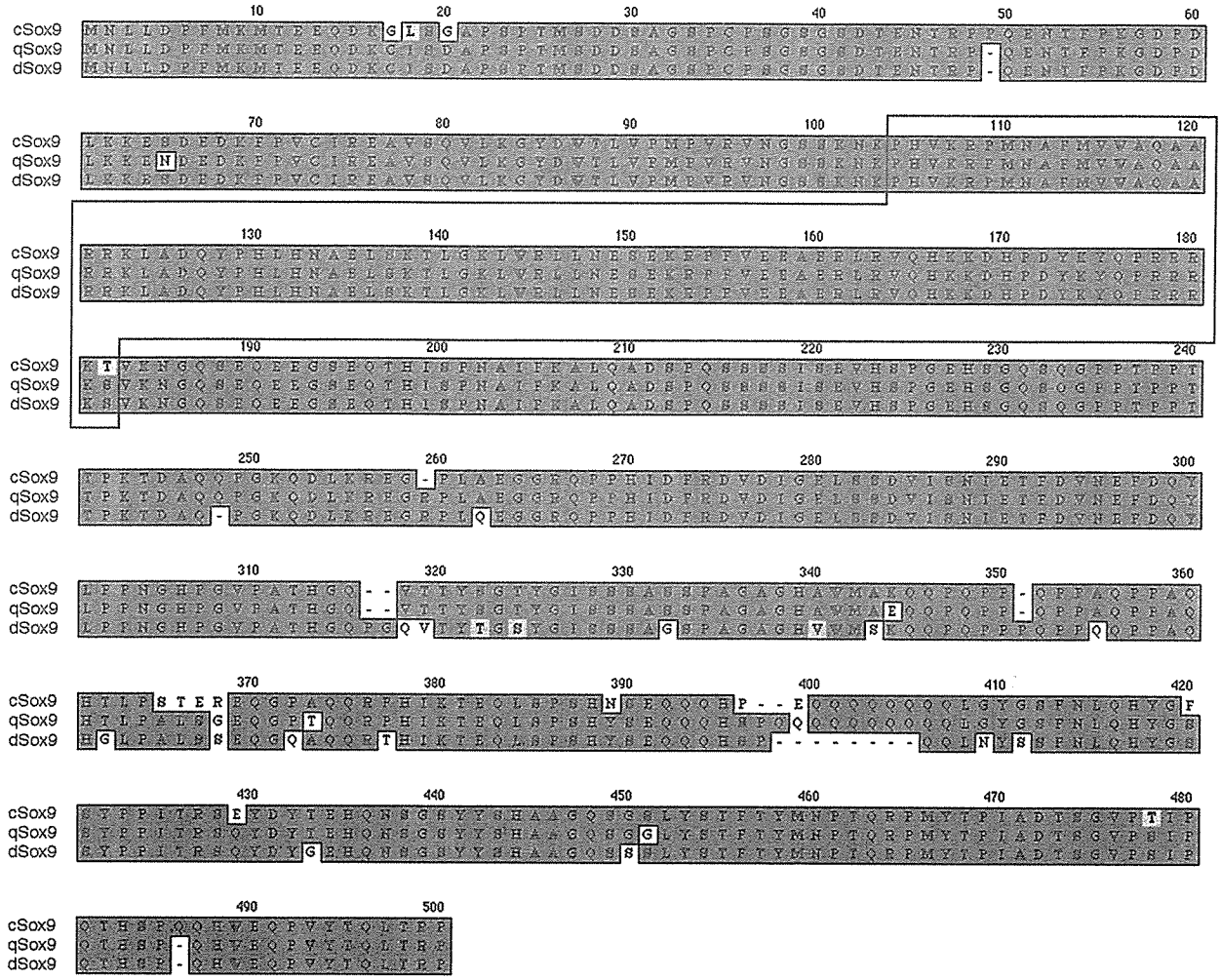

Fig. 2. Alignment of the deduced amino acid sequences of chicken (c), quail (q), and duck (d) Sox9. Dark and light gray shadings indicate identical and similar amino acids, respectively. The boxed region corresponds to the *Sry*-type HMG-box.

those of chicken Sox9 and that BLASTP searches of GenBank nonredundant database with the deduced amino acid sequences of the quail and duck proteins as queries yielded chicken and alligator Sox9 as the most similar sequences, we conclude that the isolated quail and duck cDNAs are derived from the corresponding *Sox9* genes (*qSox9* and *dSox9*, respectively). The nucleotide sequences of these cDNAs have been deposited in GenBank under the Accession Nos. AY904048 for *qSox9* and AY904046 for *dSox9*.

3.3. Expression of Sox9 in developing gonads of quail and duck

We examined the temporal and spatial expression patterns of quail and duck *Sox9* during the early stages of gonadal differentiation by whole-mount in situ hybridization with gonad–mesonephros complexes isolated from quail embryos on days 4, 5, 6, and 7 (Zacchei stages 17–18, 20–21, 22, and 24, respectively) (Zacchei, 1961) and from duck embryos on days 6, 7, 8, and 9. Duck embryos were staged by comparison with chicken (Hamburger and Hamilton, 1951); the morphological stages of duck are similar to those of chicken, although development is slightly delayed in duck (days 6, 7, 8, and 9 for duck embryos correspond to Hamburger and Hamilton stages 25–26, 28, 29–30, and 31–32, respectively).

Sox9 mRNA was not detected in quail gonads on day 4 (Figs. 3A and E) or in duck gonads on day 6 (Figs. 3J and N). *Sox9* was expressed at higher levels in male gonads than in female gonads of quail on days 5, 6, and 7 (Figs. 3B–D and F–H) as well as of duck on days 7, 8, and 9 (Figs. 3K–M and O–Q). Sense control probes yielded no specific labeling (Figs. 3I and R). The earliest detectable stages for the male-specific expression of *Sox9* were thus similar for chicken (stages 28–30) (Loffler et al., 2003; Morais da Silva et al., 1996; Oréal et al., 1998; Smith et al., 1999), quail (day 5 corresponds to Zacchei stages 20–21 and Hamburger and Hamilton stages 27–29) (Zacchei, 1961), and duck (day 7 corresponds to Hamburger and Hamilton stage 28). The expression patterns of *Sox9* in the gonads of these three avian species are also similar to that in mouse (Kent et al., 1996; Loffler et al., 2003; Morais da Silva et al., 1996; Oréal et al., 1998; Smith et al., 1999).

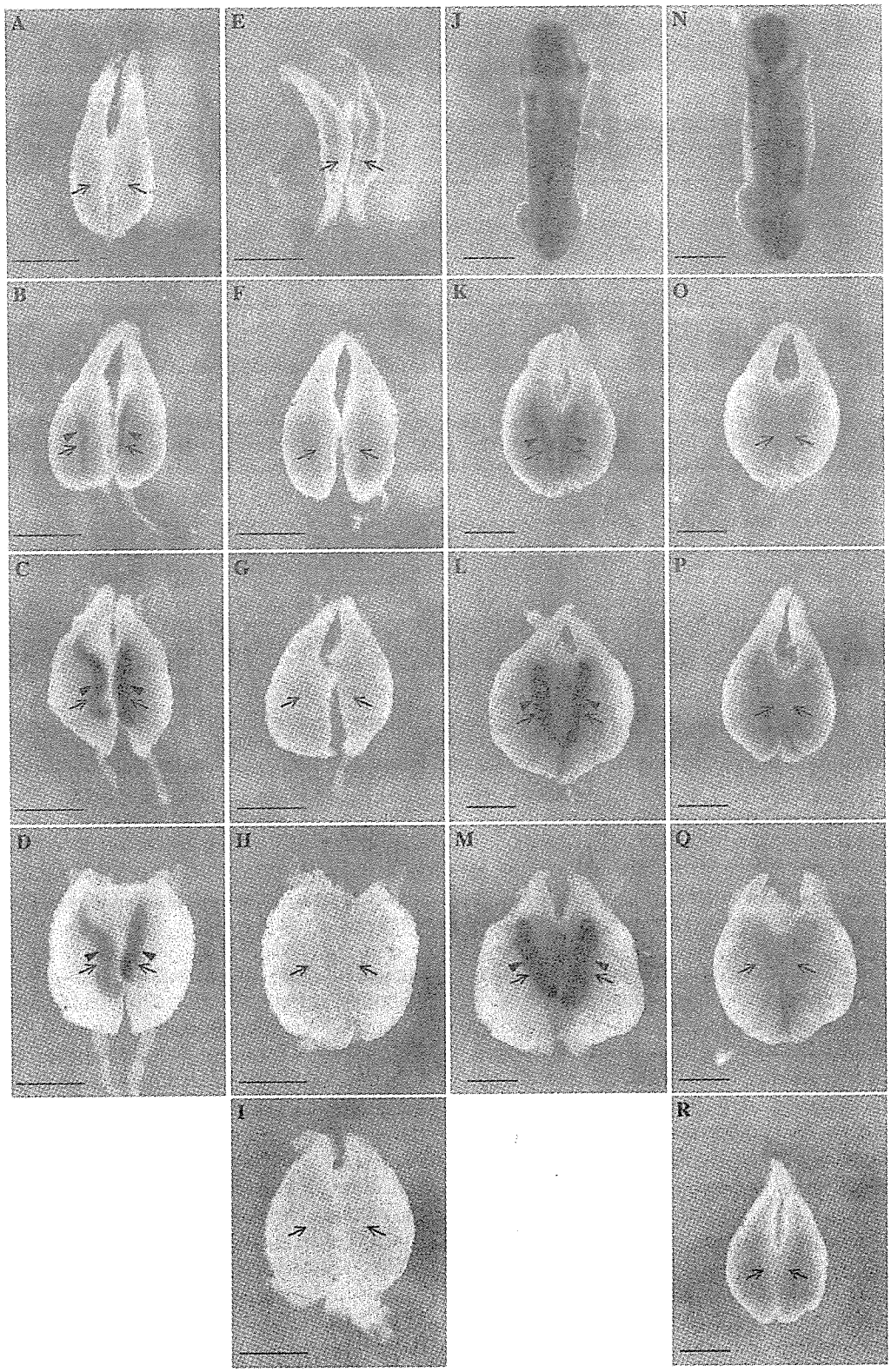

Fig. 3. Whole-mount in situ hybridization analysis of *qSox9* and *dSox9* expression in the embryonic gonad–mesonephros of quail and duck, respectively. Male (A–D and I) and female (E–H) quail embryos were analyzed on day 4 (A and E), day 5 (B and F), day 6 (C, G, and I), and day 7 (D and H). Male (J–L and M) and female (N–R) duck embryos were analyzed on day 6 (J and N), day 7 (K, O, and R), day 8 (L and P), and day 9 (M and Q). All embryos were subjected to hybridization with an antisense probe, with the exception of that in (I and R), for which a sense probe was used as a control. Arrows indicate the position of the gonad. Arrowheads indicate the region of staining. Scale bar, 1 mm.

The similarities of *Sox9* expression patterns between birds and mammals suggest that Sox9 has conserved functions in the differentiation of the embryonic gonads toward testes or ovaries. It has been postulated that Sox9 has more than one target in gonads. One of them in mammals is *Amh*, however previous studies suggested it is not a target in birds (Oréal et al., 1998; Smith et al., 1999; Takada et al., 2005). Another target in mammals identified so far is KIAA0800, which is preferentially expressed in testis while the function of which is not known (Zhao et al., 2002). Although it is not known whether KIAA0800 is expressed in avian embryonic testes or not, it can be possible that this gene and/or other genes which play a role in gonadal differentiation are regulated by Sox9 in avian and mammalian gonads. It is important to identify the targets of Sox9 in birds to understand how different hormones are produced in gonads between males and females.

In summary, the developmental expression of *qSox9* and *dSox9* is associated with testis differentiation. In quail embryos, a difference in gonadal expression of *Sox9* between the sexes was first apparent on day 5 (stages 20–21), indicating that sexual differentiation occurs at or before day 5 of incubation. In duck embryos, sexually dimorphic expression of *Sox9* was first apparent on day 7, showing that testis differentiation begins at the molecular level no later than day 7. Finally, given the similarity in the temporal and spatial expression patterns of *Sox9* during gonadogenesis in chicken, quail, and duck, comparative analysis of the *Sox9* promoters among these species may provide insight into the molecular events of sex determination or differentiation in birds.

Acknowledgments

We thank Kyoko Nakamura and Sayaka Aoyagi for assistance.

References

Clinton, M., 1998. Sex determination and gonadal development: a bird's eye view. J. Exp. Zool. 281, 457–465.

Clinton, M., Haines, L., Belloir, B., McBride, D., 2001. Sexing chick embryos: a rapid and simple protocol. Br. Poult. Sci. 42, 134–138.

Elbrecht, A., Smith, R.G., 1992. Aromatase enzyme activity and sex determination in chickens. Science 255, 467–470.

Frohman, M.A., Dush, M.K., Martin, G.R, 1988. Rapid production of full-length cDNAs from rare transcripts: amplification using a single gene-specific oligonucleotide primer. Proc. Natl. Acad. Sci. USA 85, 8998–9002.

Hamburger, V., Hamilton, H.L., 1951. A series of normal stages in the development of the chick embryo. J. Morphol. 88, 49–92.

Henke, W., Herdel, K., Jung, K., Schnorr, D., Loening, S.A., 1997. Betaine improves the PCR amplification of GC-rich DNA sequences. Nucleic Acids Res. 25, 3957–3958.

Hori, T., Asakawa, S., Itoh, Y., Shimizu, N., Mizuno, S., 2000. Wpkci, encoding an altered form of PKCI, is conserved widely on the avian W chromosome and expressed in early female embryos: implication of its role in female sex determination. Mol. Biol. Cell 11, 3645–3660.

Kent, J., Wheatley, S.C., Andrews, J.E., Sinclair, A.H., Koopman, P., 1996. A male-specific role for SOX9 in vertebrate sex determination. Development 122, 2813–2822.

Koopman, P., Gubbay, J., Vivian, N., Goodfellow, P., Lovell-Badge, R., 1991. Male development of chromosomally female mice transgenic for Sry. Nature 351, 117–121.

Loffler, K.A., Zarkower, D., Koopman, P., 2003. Etiology of ovarian failure in blepharophimosis ptosis epicanthus inversus syndrome: FOXL2 is a conserved, early-acting gene in vertebrate ovarian development. Endocrinology 144, 3237–3243.

Morais da Silva, S., Hacker, A., Harley, V., Goodfellow, P., Swain, A., Lovell-Badge, R., 1996. Sox9 expression during gonadal development implies a conserved role for the gene in testis differentiation in mammals and birds. Nat. Genet. 14, 62–68.

O'Neill, M., Binder, M., Smith, C., Andrews, J., Reed, K., Smith, M., Millar, C, Lambert, D., Sinclair, A., 2000. ASW: a gene with conserved avian W-linkage and female specific expression in chick embryonic gonad. Dev. Genes Evol. 210, 243–249.

Oréal, E., Pieau, C., Mattei, M.G., Josso, N., Picard, J.-Y., Carré-Eusèbe, D., Magre, S., 1998. Early expression of AMH in chicken embryonic gonads precedes testicular SOX9 expression. Dev. Dyn. 212, 522–532.

Smith, C.A., Smith, M.J., Sinclair, A.H., 1999. Gene expression during gonadogenesis in the chicken embryo. Gene 234, 395–402.

Spotila, L.D., Spotila, J.R., Hall, S.E., 1998. Sequence and expression analysis of WT1 and Sox9 in the red-eared slider turtle, *Trachemys scripta*. J. Exp. Zool. 281, 417–427.

Takada, S., Mano, H., Koopman, P., 2005. Regulation of *Amh* during sex determination in chickens: *Sox* gene expression in male and female gonads. Cell. Mol. Life Sci. 62, 2140–2146.

Vidal, V.P., Chaboissier, M.C., de Rooij, D.G., Schedl, A., 2001. Sox9 induces testis development in XX transgenic mice. Nat. Genet. 28, 216–217.

Xu, Q., Wilkinson, D., 1998. In situ hybridisation of mRNA with hapten labelled probes. In: Wilkinson, D. (Ed.), In Situ Hybridisation: A Practical Approach, second ed. Oxford University Press, Oxford, pp. 87–106.

Zacchei, A.M., 1961. The embryonal development of the Japanese quail (*Coturnix coturnix japonica* T. and S.). Arch. Ital. Anat. Embryol. 66, 36–62.

Zhao, L.J., Zhang, S., Chinnadurai, G., 2002. Sox9 transactivation and testicular expression of a novel human gene, KIAA0800. J. Cell. Biochem. 86, 277–289.

Published online 14 September 2006

Nucleic Acids Research, 2006, Vol. 34, No. 17 ***e115***
doi:10.1093/nar/gkl653

Mouse microRNA profiles determined with a new and sensitive cloning method

Shuji Takada[1], Eugene Berezikov[2], Yoshihiro Yamashita[1], Mariana Lagos-Quintana[3], Wigard P. Kloosterman[2], Munehiro Enomoto[1], Hisashi Hatanaka[1], Shin-ichiro Fujiwara[1], Hideki Watanabe[1], Manabu Soda[1], Young Lim Choi[1], Ronald H. A. Plasterk[2], Edwin Cuppen[2] and Hiroyuki Mano[1,4,*]

[1]Division of Functional Genomics, Jichi Medical University, 3311-1 Yakushiji, Shimotsukeshi, Tochigi 329-0498, Japan, [2]Hubrecht Laboratory, Uppsalalaan 8, Utrecht, The Netherlands, [3]Laboratory of RNA Molecular Biology, Rockefeller University, 1230 York Avenue, New York, NY 10021, USA and [4]CREST, Japan Science and Technology Agency, Saitama 332-0012, Japan

Received August 8, 2006; Revised August 14, 2006; Accepted August 19, 2006

ABSTRACT

MicroRNAs (miRNAs) are noncoding RNA molecules of 21 to 24 nt that regulate the expression of target genes in a post-transcriptional manner. Although evidence indicates that miRNAs play essential roles in embryogenesis, cell differentiation and pathogenesis of human diseases, extensive miRNA profiling in cells or tissues has been hampered by the lack of sensitive cloning methods. Here we describe a highly efficient profiling method, termed miRNA amplification profiling (mRAP), as well as its application both to mouse embryos at various developmental stages and to adult mouse organs. A total of 77 436 Small-RNA species was sequenced, with 11 776 of these sequences found to match previously described miRNAs. With the use of a newly developed computational prediction algorithm, we further identified 229 independent candidates for previously unknown miRNAs. The expression of some of these candidate miRNAs was confirmed by northern blot analysis and whole-mount *in situ* hybridization. Our data thus indicate that the total number of miRNAs in vertebrates is larger than previously appreciated and that the expression of these molecules is tightly controlled in a tissue- and developmental stage-specific manner.

INTRODUCTION

MicroRNAs (miRNAs) are short noncoding RNA molecules that inhibit gene expression through incomplete base pairing with the 3′-untranslated region (3′-UTR) of target mRNAs (1,2). The miRNA system is conserved from worms to mammals and contributes to the regulation of a wide variety of cellular functions. In *Caenorhabditis elegans*, for instance, larval development is regulated by a set of miRNAs that include members of the *lin-4* and *let-7* families (3,4), and the function of *Dicer1*, which encodes an enzyme essential for miRNA biogenesis, is indispensable for mouse embryonic development (5). Furthermore, the miRNA miR-181 has been implicated in the differentiation of mouse B lymphocytes (6).

Evidence indicates that miRNAs also play a role in the pathogenesis of human disorders including cancer. The expression profiles of miRNAs are thus effective for classification of human cancers (7,8). Human *let-7* miRNAs target transcripts of the proto-oncogene RAS and are down-regulated in a large proportion of lung cancer specimens (9). Localization of miRNA genes to the fragile sites of human chromosomes indicates that many more miRNAs may be linked to carcinogenesis (10).

Although the recent public miRNA registry (miRBase release 7.1 at http://microRNA.sanger.ac.uk) contains 326 entries for human miRNAs, a large number of additional human miRNAs are thought to exist (11,12). Given the relation of miRNAs to cell growth and differentiation and to human disease, it is important to compare the expression profiles of miRNAs (both known and unidentified previously) among normal tissues and clinical specimens. Such studies have been hampered, however, by the lack of sensitive cloning methods for miRNAs. Current standard procedures for miRNA isolation require several 100 μg of total RNA as a starting material (13), an amount that is difficult to obtain from small tissues or clinical specimens. To overcome such limitations, we have developed a highly sensitive cloning method for miRNAs, which we have termed miRNA amplification profiling (mRAP).

*To whom correspondence should be addressed. Tel: +81 285 58 7449; Fax: +81 285 44 7322; Email: hmano@jichi.ac.jp

MATERIALS AND METHODS

mRAP

A Small-RNA fraction was directly isolated from cells with the use of a mirVana miRNA Isolation Kit (Ambion). In our experience, the yield of Small-RNA with this kit was about 40–50% of that for total RNA obtained by conventional methods from the same number of cells. A portion of this Small-RNA fraction together with size markers (19, 24 and 33 nt) was subjected to electrophoresis on a 15% polyacrylamide gel under denaturing conditions. The region of the gel containing RNA of 19–24 nt was excised, and the RNA molecules were recovered, dephosphorylated by incubation for 30 min at 50°C with calf intestinal alkaline phosphatase (New England Biolabs) and ligated to the 3′ adaptor [5′-(Pu)uuAACCGCGAATTCCAG(idT)-3′], where lowercase letters indicate RNA, uppercase letters indicate DNA, Pu denotes 5′-phosphorylated uridine, and idT represents 3′-inverted deoxythymidine (Dharmacon). The ligated RNA was subjected to reverse transcription with PowerScript reverse transcriptase (Clontech) and the RT primer (5′-GACTAGCTGGAATTCGCGGTTAAA-3′) in the presence of the 5′ adaptor (5′-GACCACGCGTATCGGGCACCACGTATGCTATCGATCGTGAGATGGG-3′). The products were amplified by PCR for 32 cycles of incubation at 95°C for 30 s and 65°C for 30 s with AmpliTaq Gold DNA polymerase (Applied Biosystems), the 5′ PCR primer (5′-GCGTATCGGGCACCACGTATGC-3′), and the 3′ PCR primer (5′-GACTAGCTTGGTGCCGAATTCGCGGTTAAA-3′). The resulting amplicons were fractionated by electrophoresis, and those from 90 to 95 bp were eluted, digested with BanI endonuclease (New England Biolabs), and subjected to concatamerization with the use of a Ligation High Kit (Toyobo, Osaka, Japan). Products from 500 to 2000 bp were isolated by electrophoresis and cloned into the pGEM-Teasy vector (Promega). A more detailed description of the mRAP protocol is provided as Supplementary Data on the NAR web site.

Prediction of novel miRNAs

Base calling and quality trimming of sequence chromatograms were performed with phred software (14). After masking of vector and adaptor sequences and removal of redundancy, inserts of ≥18 bp were mapped to genomes (ncbi35 assembly for human, ncbim34 assembly for mouse) with the use of the megablast program in the NCBI software suite (ftp://ftp.ncbi.nlm.nih.gov/blast). For every genomic locus that matched an insert, repeat annotations were retrieved from the Ensembl database (http://www.ensembl.org) and repetitive regions were discarded. Genomic regions containing inserts with 100 nt flanking sequences were retrieved from Ensembl, and a sliding window of 100 nt was used to calculate RNA secondary structures with RNAfold software from the Vienna RNA Secondary Structure Package (15).

To detect homologous hairpins in other genomes, we performed a BLAST search with mature regions of each RNA sequence against human, mouse, rat, dog, cow, opossum, chicken, zebrafish and fugu genomes. Hits of ≥20 nt with an identity of ≥70% were extracted from the genomes together with flanking sequences of a size similar to that observed for the original hairpins. Extracted sequences were checked for hairpin structures with the use of RNAfold, and positive hairpins were aligned with the original hairpin with CLUSTAL W (16). For remaining hairpins, randfold (17) values were calculated for every sequence in an alignment by mononucleotide shuffling and 1000 iterations. A cutoff of 0.01 was used for randfold, and only regions that contained a hairpin below this cutoff for at least one species in an alignment were considered as candidates of miRNA genes. Berezikov *et al.* (18) describe the computational method for prediction of miRNAs in more detail.

Northern blot analysis

Small-RNA fractions (0.1 to 0.5 μg) were subjected to electrophoresis on a 15% polyacrylamide gel under denaturing conditions, and the separated molecules were transferred electrophoretically to a Hybond-N nylon membrane (Amersham Biosciences). The membrane was incubated with ^{32}P-labeled locked nucleic acid (LNA) corresponding to mature miRNA sequences in ULTRAhyb-Oligo solution (Ambion), and signals were detected with a BAS-1500 image analyzer (Fuji Photo Film).

Whole-mount *in situ* hybridization

Whole-mount *in situ* hybridization was performed as described (19). LNA-modified oligonucleotides were synthesized by Thermo Electron (Ulm, Germany), and digoxigenin labeling was performed with a DIG Oligonucleotide 3′ End Labeling Kit (Roche Diagnostics, Penzberg, Germany).

RESULTS

Development of mRAP

To isolate miRNAs from small quantities of RNA, we first tried to amplify the miRNA fraction by incorporating simple PCR steps into the conventional miRNA cloning procedures (13). However, all such trials resulted in an amplification of non-specific products from degraded RNAs and adaptor-primer concatamers without miRNA-derived cDNAs (as shown in Figure 1A). To circumvent this limitation, we invented the mRAP procedure by utilizing (1) the SMART method (Clontech) for an efficient cDNA amplification and (2) a long, sophisticated 5′ adaptor. All nucleotide sequences of the 5′ adaptor originally invented by Lagos-Quintana (13), SMART IIA oligonucleotide (Clontech), and a BanI site (for a uni-directional concatamerization of PCR products) were incorporated into our initial 5′ adaptor sequence, which was subsequently optimized by addition/removal of nucleotides to reduce non-specific PCR products. In addition, the length of the 5′ adaptor (46 bases) was determined so that the miRNA-derived products can be easily separated from the two major byproducts (see Figure 1A).

In the mRAP procedure, isolated Small-RNA molecules are first ligated at their 3′ end to a 3′ adaptor and then reverse-transcribed with the use of a primer (RT primer) complementary to the 3′ adaptor (Figure 1A). Because of the fact that certain reverse transcriptases possess terminal deoxynucleotidyl transferase activity a few nucleotides

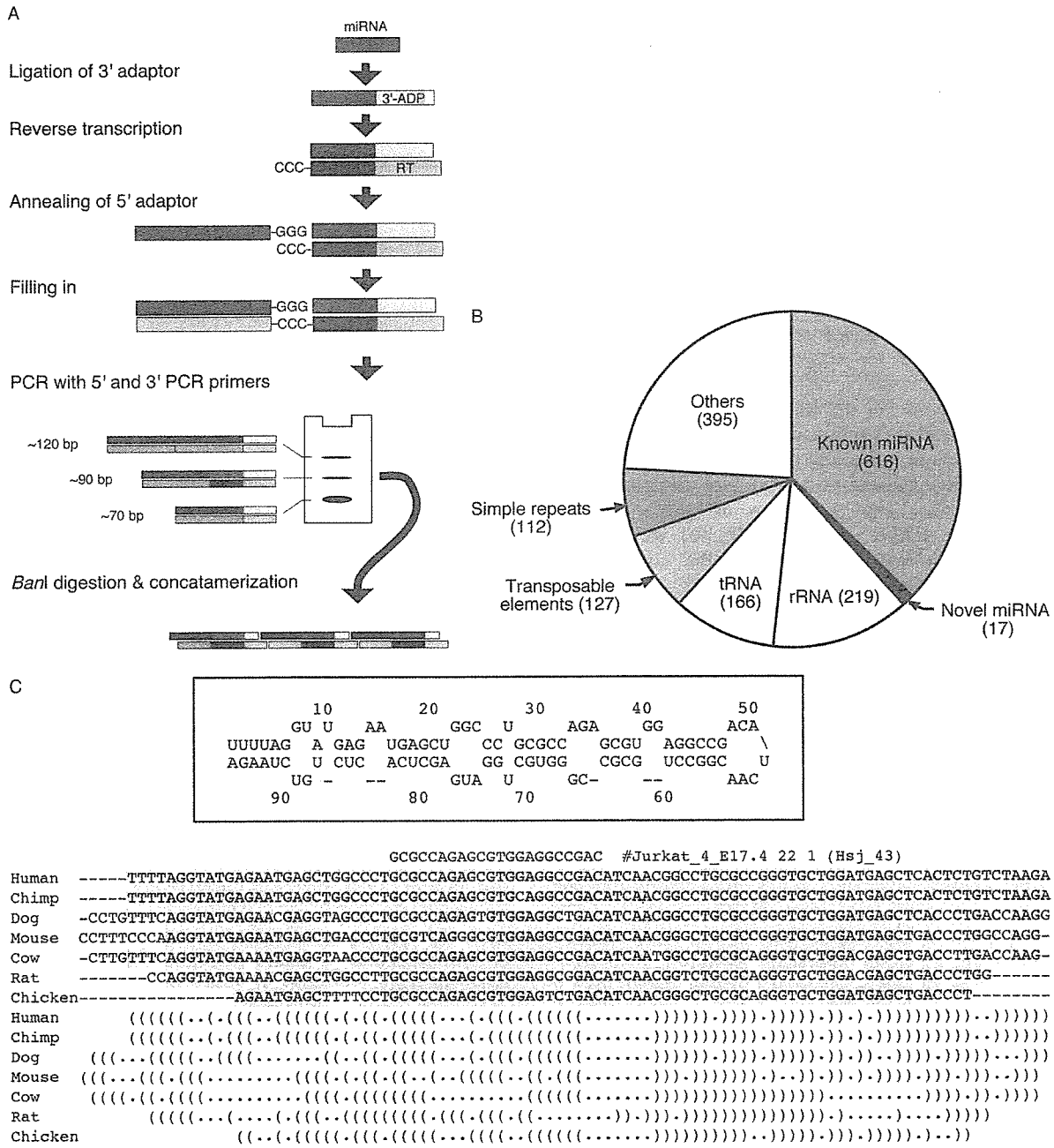

Figure 1. The mRAP protocol and its application to Jurkat cells. (**A**) Isolated Small-RNA molecules are ligated to the 3′ adaptor (3′-ADP) and subjected to reverse transcription with the RT primer. After annealing of the 5′ adaptor (5′-ADP) to the poly(C) overhang at the 3′ end of the synthesized cDNAs, the latter are subjected to PCR with the 5′ and 3′ PCR primers. After an extensive cloning/sequencing of the PCR products, we noticed that, of the three major sizes of amplicon generated, only the middle one includes cDNAs derived from miRNAs. The large product of ~120 bp is composed of two 5′ adaptors and one 3′ adaptor without miRNA sequences. The small product of ~70 bp is, on the other hand, composed of only one 5′ adaptor and one 3′ adaptor. The product of ~90 bp are thus isolated, digested with BanI, and self-ligated to yield concatamers. (**B**) Among 1652 mRAP clones of Jurkat cells that matched the human genome sequence, 616 clones corresponded to known miRNAs, 17 are candidates for novel miRNAs and 219 corresponded to rRNAs, 166 to tRNAs, 127 to transposable elements, 112 to simple repeats and 395 to other genomic sequences that do not fold into a hairpin or otherwise fail the miRNA prediction pipeline. (**C**) Alignment of the nucleotide sequence (red) of one predicted novel miRNA (Hsj_43) with genomic sequences of human, chimpanzee, dog, mouse, cow, rat and chicken. Nucleotides conserved between human and other species are shaded in gray. Possible base pairing schemes for the respective Hsj_43 precursors are shown below the aligned sequences and, for the human sequence, in the upper inset.

(mostly deoxycytidine) are added to the 3′ end of each cDNA strand (20). After the annealing of a 5′ adaptor to the poly(C) overhang of the cDNAs, PCR is performed with 5′ and 3′ PCR primers to exponentially amplify the cDNAs. The isolated cDNAs are digested with the BanI restriction endonuclease and self-ligated to generate concatamers, which are then inserted into a plasmid vector for nucleotide sequencing.

As a test case, we first applied mRAP to 5 μg of a Small-RNA fraction isolated from the human T cell line Jurkat. The procedure readily generated >1 × 10^4 colony-forming units of the concatamer library. A total of 958 clones was randomly chosen from the library and subjected to nucleotide sequencing. Each plasmid insert consisted of multiple short cDNAs (average of 2.59 cDNAs per insert), and the dataset contained a total of 2392 such cDNAs of ⩾18 bp. The 1652 cDNA sequences that passed quality assessment were subjected to computational screening for previously unidentified miRNAs with an algorithm developed in-house. In brief, after filtering of repeat, rRNA, tRNA and small nucleolar (snoRNA) sequences, the remaining sequences predicted to fold into stable stem–loop structures were selected and checked for overlap with known miRNA genes (18).

As shown in Figure 1B, the Jurkat dataset contained 616 clones of known miRNAs (corresponding to 60 independent miRNAs) and 17 clones of newly predicted miRNAs (corresponding to 15 independent miRNAs) (see Supplementary Tables S1 and S2). The proportion of miRNA clones among our Jurkat cDNA sequences (38.3%) was slightly smaller than that (46.9%) obtained by the conventional method by Lagos-Quintana *et al.* (13).

One such candidate for the novel miRNA sequences ('Hsj_43' according to our tentative nomenclature system) is shown aligned with vertebrate genomes in Figure 1C. The precursor of this miRNA is presumed to comprise 95 nt in human, and its nucleotide sequence is conserved among various vertebrates and can fold into an incompletely complementary hairpin structure (Figure 1C).

To determine whether mRAP is able to efficiently isolate miRNAs from a small number of cells, we prepared a Small-RNA fraction (7 μg, 700 and 70 ng, respectively) from 1 × 10^6, 1 × 10^5 and 1 × 10^4 Jurkat cells. We found that mRAP readily generated >1 × 10^4 colony-forming units of concatamer libraries from all three samples (data not shown). Nucleotide sequencing of randomly chosen clones revealed that the most abundant hsa-miR-142-3p occupies 36.6% (26 reads out of 71 total miRNA reads), 26.1% (24 out of 92) and 20.0% (17 out of 85) of total miRNA clones isolated from the 1 × 10^6, 1 × 10^5 and 1 × 10^4 cells, respectively (data not shown). Similarly, another abundant miRNA, hsa-miR-143, could be found in 11.3% (8 reads), 9.8% (9 reads) and 15.3% (13 reads) of miRNAs from the 1 × 10^6, 1 × 10^5 and 1 × 10^4 cells, respectively. The proportion of isolated rRNAs was also constant among the samples, indicating the high fidelity of mRAP even when performed with a small number of cells. These data confirmed that mRAP is highly sensitive for characterization of miRNA profiles, needing <0.1% of the initial RNA quantity required for current methods (13).

miRNA profiling of mouse embryos

We next applied mRAP to obtain miRNA profiles of mouse. We first isolated mouse embryos at 6.5, 7.5, 8.5, 9.5, 10.5, 11.5, 12.5, 13.5, 14.5, 15.5 and 17.5 days postcoitum (dpc) and subjected them to miRNA profiling. A total of 25 944 small cDNAs was sequenced for all embryos (average of 2359 clones per embryo); 3362 of these clones corresponded to 150 known miRNAs (miRBase release 7.1), and 198 of them corresponded to 75 novel miRNAs (see Supplementary Tables S3 and S4). These data indicated that many miRNAs are expressed from an early stage of embryogenesis (at 6.5 dpc, for instance, 9.63% of Small-RNA species corresponded to miRNAs). Furthermore, novel candidate miRNAs were detected throughout embryogenesis; the proportion of novel miRNAs among all known and unknown miRNAs was 6.54 ± 3.67% (mean ± SD) for the developmental stages examined.

The expression profiles of miRNAs at each developmental stage of the mouse embryo are summarized in Figure 2A and Supplementary Table S3. Whereas some miRNAs, (such as mmu-mir-124a) are expressed throughout embryonic development, many others are expressed only at specific stages. Expression of mmu-mir-206, e.g. was almost undetectable up to 13.5 dpc but was increased markedly at 14.5 dpc and thereafter. Expression of mmu-mir-148a was largely restricted to 10.5 dpc, at which time it constituted 16.07% of all miRNAs. Similarly, 24 cDNA clones (7.55% of all miRNA species) derived from the mouse embryo at 7.5 dpc corresponded to mmu-mir-23b, whereas only 0 to 3 such clones were identified at other stages of development.

We performed Northern blot analysis to confirm the miRNA profiles identified by mRAP screening. As shown in Figure 2B, northern analysis revealed that the expression of mmu-mir-206 increased progressively with time of embryonic development, whereas that of mmu-mir-124a remained relatively stable (with a slight increase apparent at 13.5 to 15.5 dpc). Direct comparison revealed that the temporal profiles of mmu-mir-206 expression determined by northern blot analysis and by mRAP were similar, with a slight difference in detection sensitivity (Figure 2C).

Northern analysis also detected the putative novel miRNA Mmj_157 at an appropriate size and with preferential expression in mid to late stages of embryogenesis (Figure 2B). We examined the localization of putative miRNAs in whole-mount preparations of mouse embryos at 10.5 dpc by *in situ* hybridization with LNA-modified DNA as a probe. Some of the novel miRNAs were found to be expressed in a tissue-specific manner. Both Mmj_163 and Mmj_157 putative miRNAs were detected specifically in the central nervous system, with the former being preferentially expressed in the telencephalon and the latter in the myelencephalon (Figure 2D). Despite its abundance in the central nervous system of embryos, we were not able to detect Mmj_157 in adult brain (Figure 3A and Supplementary Table S5), indicating that expression of this putative miRNA is both spatially and temporally restricted. In adult mice, a substantial amount of Mmj_157 was apparent only in the placenta, in which it constituted 12.85% of all miRNA clones.

miRNA profiling of adult mouse organs

We next determined the miRNA profiles for 21 organs of the adult mouse with the mRAP procedure. A total of 51 492 clones derived from Small-RNAs (average of 2452 clones per organ) was sequenced and found to include 8141 clones of known miRNAs and 287 clones of novel candidate miRNAs. The distribution of abundant miRNAs in each organ is shown schematically in Figure 3A, with the complete

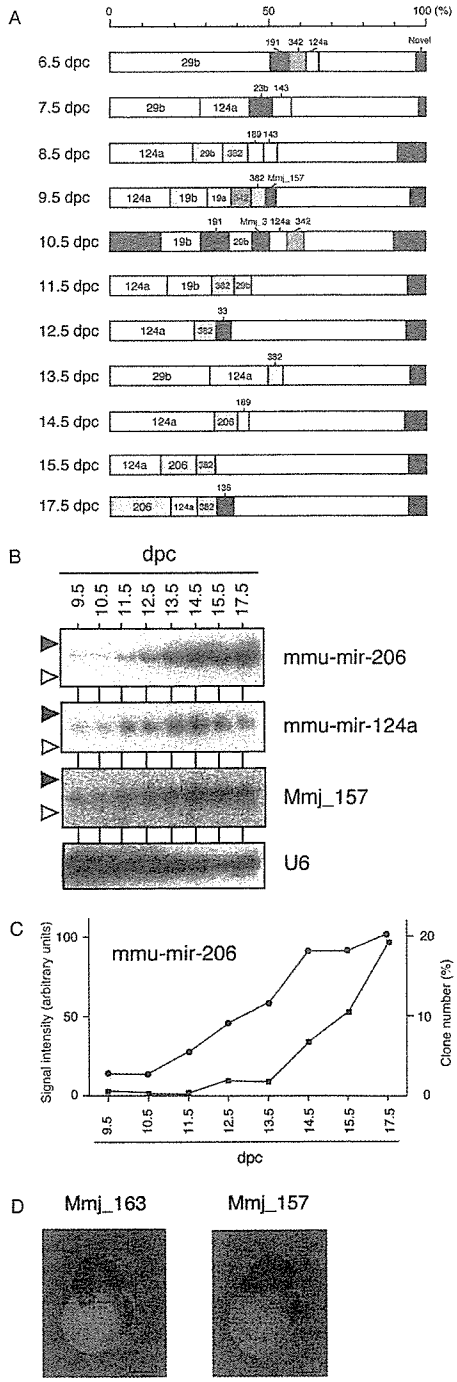

Figure 2. Expression profiles of miRNAs in the mouse embryo. (**A**) The percentage of each miRNA among the total miRNA population was calculated for mouse embryos at the indicated stages of development (6.5 to 17.5 dpc). Abundant miRNAs are shown color-coded, with candidates for novel miRNAs in red. (**B**) Northern blot analysis of the Small-RNA fraction isolated from mouse embryos at the indicated developmental stages (9.5 to 17.5 dpc). The blot was probed with oligonucleotides specific for mmu-mir-206, mmu-mir-124a or Mmj_157; a probe for U6 small nuclear RNA was used as an internal control. Closed and open arrowheads indicate the positions of 24 and 19 nt, respectively. (**C**) Expression level of mmu-mir-206 during mouse embryogenesis as determined from the northern blot in (B) (red line) and from the mRAP dataset (blue line). (**D**) Whole-mount *in situ* hybridization of mouse embryos at 10.5 dpc with LNA-modified probes specific for Mmj_163 or Mmj_157. Scale bar, 1 mm.

dataset being presented in Supplementary Table S5. Some miRNAs, including mmu-mir-124a and mmu-mir-143, were found to be expressed ubiquitously among organs, whereas many others were abundant in only a subset of organs, with their relative expression (clone number) varying markedly among such organs. Marked expression of mmu-let-7b, for example, was apparent only in kidney, lung and ovary, and the proportion of mmu-mir-382 among all miRNA clones was >1% only in brain and placenta.

Candidates for novel miRNAs were found in the proportion of 4.20 ± 4.75% (mean ± SD) of all miRNA species for each organ. Similar to known miRNAs, expression of these candidate miRNAs was found to be regulated in a tissue-dependent manner (Supplementary Table S5). We did not detect a correlation between the miRNA profiles and germ-layer origins of organs.

Northern blot analysis confirmed the organ-specific expression of known and novel miRNAs in the adult mouse (Figure 3B). Expression of Mmj_157 was found to be restricted to the placenta and ovary, consistent with the mRAP data (Figure 3C). Northern analysis revealed expression of mmu-mir-122a to be largely liver-specific (with a low level of expression also apparent in stomach), again consistent with the expression profile obtained by mRAP (Figure 3B and C).

DISCUSSION

We have thus developed a sensitive method for miRNA profiling and have applied this method to obtain the first extensive miRNA profiles of the mouse. Our screening identified 229 putative novel miRNAs (corresponding to 260 loci on mouse chromosomes). Sequence conservation of our novel miRNA candidates among different species is summarized in Supplementary Table S6. In compliance with criteria for miRNA annotation, we require several independent lines of experimental evidence (e.g. cloning and northern blot analysis, or cloning from several libraries) to define a novel miRNA as a bona fide miRNA (21,22). If experimental evidence is limited (e.g. cloned only from one library), novel miRNAs are considered as candidates and are annotated correspondingly (Supplementary Table S7).

It should be noted that, since three Gs are added to the 5′-termini of miRNAs in mRAP (Figure 1A), it might be difficult to precisely determine the 5′ ends of miRNAs especially when the genomic sequence adjacent to mature miRNAs contains Gs. Thus, it is possible that the nucleotide sequences of our novel miRNA candidates in Supplementary Tables S2 and S4 will contain inappropriate Gs at the 5′-termini.

Although, we sequenced 77 436 mouse Small-RNA species, many miRNAs were isolated only once in each tissue or embryo (Supplementary Tables 3 and 5), suggesting that the overall mouse miRNA catalog may not have been fully revealed. Furthermore, given the stringent parameters in our computational screening, it is possible that some bona fide novel miRNAs in our dataset were inappropriately dropped at this *in silico* step. Screening for novel miRNAs by a microarray approach with the same computational algorithm identified a different, but partially overlapping, set of

candidate miRNAs in mouse (18). Similarly, our screening for miRNAs in human clinical specimens by mRAP resulted in the isolation of a set of candidate novel miRNAs that include many with no mouse orthologs either in our dataset or in the miRBase depository (S. Takada, Y. Yamashita, E. Berezikov, Y.L. Choi, S. Fujiwara, M. Enomoto, H. Hatanaka, H. Watanabe, M. Soda, R.H.A. Plasterk, E. Cuppen and H. Mano, manuscript submitted). It is thus likely that the mouse genome encodes additional miRNAs yet to be discovered.

Isolation of novel miRNAs has been attempted to date through a variety of approaches. Lagos-Quintana *et al.* (13) compared miRNA profiles among mouse organs by a conventional miRNA cloning procedure. They identified that three miRNAs are expressed in a tissue-specific manner; mmu-mir-1 in heart, mmu-mir-124a in brain and mmu-mir-122a in liver, all of which is in a very good agreement with our observation (see Figure 3A and Supplementary Table S5). On the other hand, Barad *et al.* (23) chose oligonucleotide microarrays to compare miRNA profiles among five human tissues. Again, they revealed a tissue-specific expression of hsa-miR-122a and hsa-miR-124a, which matches our results.

Mineno *et al.* (24) recently analyzed miRNA expression with the massively parallel signature sequencing (MPSS) technology among three developmental stages (9.5, 10.5 and 11.5 dpc) of mouse embryo. Many of their 'top 20 miRNA signatures' can be observed in our dataset. For instance, their result reveals that the expression of mmu-mir-199a was increased from 9.5 to 11.5 dpc of mouse embryo. Our data demonstrates that the augmentation of mmu-mir-199a expression further continues to 15.5–17.5 dpc (Supplementary Table S3) of embryo. Similarly, both of our and Mineno's data indicate that mmu-mir-19b is abundantly expressed at 9.5–11.5 dpc of mouse embryo (Supplementary Table S3). Additionally, one of the abundant novel miRNAs in our embryo dataset, Mmj_157, was also counted for many times as miRNA426 in the data of Mineno *et al.* There may be, however, some difference between these two datasets. One of the highly expressed miRNAs in mouse embryo, mmu-mir-124a, in our data are missed from that of Mineno *et al.* Our northern blot analysis in Figure 2B supports the expression of mmu-mir-124a in embryo.

To directly compare our mRAP data with those by other high-throughput methods, we then hybridized RNA from

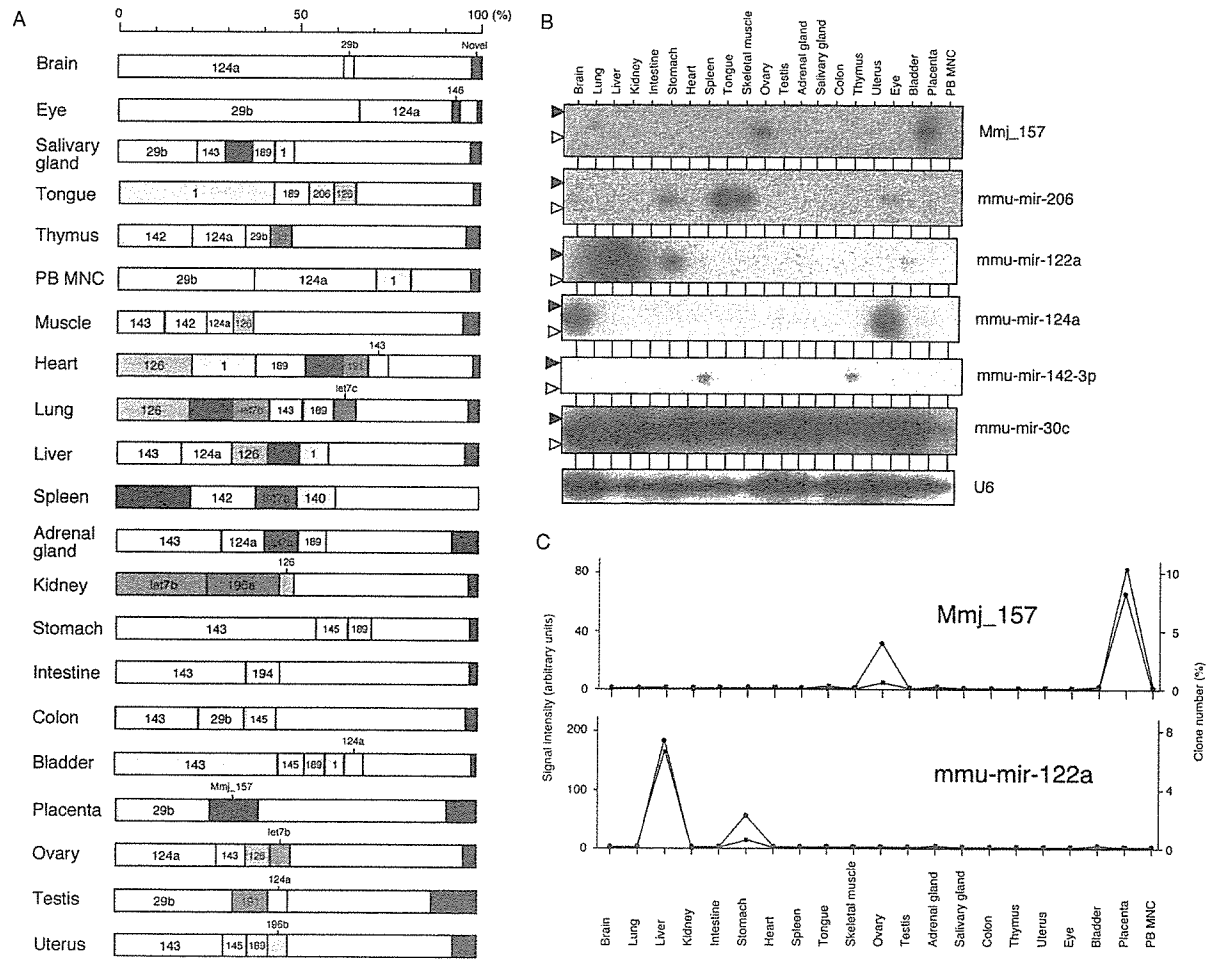

Figure 3. Expression profiles of miRNAs in adult mouse organs. (A) The percentage of each miRNA among the total miRNA population was calculated for the indicated organs of the adult mouse and is shown schematically as in Figure 2A. PB MNC, peripheral blood mononuclear cells. (**B**) Northern blot analysis of the Small-RNA fraction from the indicated adult mouse organs with probes specific for the indicated RNA species. (C) Expression levels of Mmj_157 or mmu-mir-122a in adult mouse organs as determined from the northern blot in (B) and from mRAP data.

Jurkat cell line to miRCURY LNA microarrays (Exiqon, Vedbaek, Denmark) to quantitate miRNA amounts. Hsa-miR-142, the most abundant miRNA in our Jurkat dataset (Supplementary Table S1), was indeed identified as one of the strongest signals in the array data (data not shown). However, with regard to another abundant miRNA hsa-miR-143 in our dataset, the microarray could give a hybridization signal only at the intensity of backgrounds (data not shown). Northern blot analysis clearly confirmed the expression of hsa-miR-143 in Jurkat cells (Supplementary Figure S1), supporting our mRAP data. Caution should thus be taken to estimate the miRNA profiles based on some type of microarrays.

We also quantitated the expression level of mmu-mir-122a, mmu-mir-185 and let-7-a with the TaqMan MicroRNA assay (Applied Biosystems) in mouse brain, liver and heart. Relative expression intensity of mmu-mir-122a to that of let-7-a was 1.056×10^{-4} for brain, 7.227 for liver and 1.230×10^{-4} for heart, indicating the liver-specific expression of mmu-mir-122a. On the other hand, the TaqMan assay revealed a weak but ubiquitous expression of mmu-mir-185; its relative expression level to that of let-7-a was 5.759×10^{-3} for brain, 3.816×10^{-3} for liver and 6.769×10^{-3} for heart. Both of these data are highly compatible with our dataset (Supplementary Table S5).

Given that mRAP is able to provide an miRNA profile with as few as 1×10^4 cells, it opens up the possibility of direct characterization of miRNAs in small amounts of tissue, such as those available for mouse embryos (as demonstrated in the present study) and fresh human specimens. Indeed, with mRAP, we have characterized miRNA profiles even for small papillary muscles of the human heart ventricle (S. Takada, R. Kaneda, E. Berezikov, Y. Yamashita, Y.L. Choi, S. Fujiwara, M. Enomoto, H. Hatanaka, H. Watanabe, M. Soda, R.H.A. Plasterk, E. Cuppen and H. Mano, manuscript submitted). Our present miRNA profiling in mouse has shown that such profiles vary markedly among tissues and developmental stages. An important application of mRAP will be determination of whether expression of miRNAs is associated with human disease by analysis of fresh human tissue specimens.

SUPPLEMENTARY DATA

Supplementary Data are available at NAR online.

ACKNOWLEDGEMENTS

The authors thank K. Nakamura for help in preparation of the manuscript. This work was supported in part by a grant for Third-Term Comprehensive Control Research for Cancer from the Ministry of Health, Labor and Welfare of Japan, and by a grant for 'High-Tech Research Center' Project for Private Universities: matching Fund Subsidy from the Ministry of Education, Culture, Sports, Science and Technology of Japan (2002–2006). E.B. was supported by the Horizon Breakthrough grant from the Netherlands Genomics Initiative. Funding to pay the Open Access publication charges for this article was provided by the Ministry of Education, Culture, Sports, Science and Technology, Japan.

Conflict of interest statement. None declared.

REFERENCES

1. Meister,G. and Tuschl,T. (2004) Mechanisms of gene silencing by double-stranded RNA. *Nature*, **431**, 343–349.
2. Bartel,D.P. (2004) MicroRNAs: genomics, biogenesis, mechanism and function. *Cell*, **116**, 281–297.
3. Abbott,A.L., Alvarez-Saavedra,E., Miska,E.A., Lau,N.C., Bartel,D.P., Horvitz,H.R. and Ambros,V. (2005) The let-7 MicroRNA family members mir-48, mir-84, and mir-241 function together to regulate developmental timing in *Caenorhabditis elegans*. *Dev. Cell*, **9**, 403–414.
4. Lee,R.C., Feinbaum,R.L. and Ambros,V. (1993) The *C. elegans* heterochronic gene lin-4 encodes Small-RNAs with antisense complementarity to lin-14. *Cell*, **75**, 843–854.
5. Bernstein,E., Kim,S.Y., Carmell,M.A., Murchison,E.P., Alcorn,H., Li,M.Z., Mills,A.A., Elledge,S.J., Anderson,K.V. and Hannon,G.J. (2003) Dicer is essential for mouse development. *Nature Genet.*, **35**, 215–217.
6. Chen,C.Z., Li,L., Lodish,H.F. and Bartel,D.P. (2004) MicroRNAs modulate hematopoietic lineage differentiation. *Science*, **303**, 83–86.
7. Lu,J., Getz,G., Miska,E.A., Alvarez-Saavedra,E., Lamb,J., Peck,D., Sweet-Cordero,A., Ebert,B.L., Mak,R.H., Ferrando,A.A. *et al.* (2005) MicroRNA expression profiles classify human cancers. *Nature*, **435**, 834–838.
8. Calin,G.A., Ferracin,M., Cimmino,A., Di Leva,G., Shimizu,M., Wojcik,S.E., Iorio,M.V., Visone,R., Sever,N.I., Fabbri,M. *et al.* (2005) A MicroRNA signature associated with prognosis and progression in chronic lymphocytic leukemia. *N. Engl. J. Med.*, **353**, 1793–1801.
9. Johnson,S.M., Grosshans,H., Shingara,J., Byrom,M., Jarvis,R., Cheng,A., Labourier,E., Reinert,K.L., Brown,D. and Slack,F.J. (2005) RAS is regulated by the let-7 microRNA family. *Cell*, **120**, 635–647.
10. Calin,G.A., Sevignani,C., Dumitru,C.D., Hyslop,T., Noch,E., Yendamuri,S., Shimizu,M., Rattan,S., Bullrich,F., Negrini,M. *et al.* (2004) Human microRNA genes are frequently located at fragile sites and genomic regions involved in cancers. *Proc. Natl Acad. Sci. USA*, **101**, 2999–3004.
11. Berezikov,E., Guryev,V., van de Belt,J., Wienholds,E., Plasterk,R.H. and Cuppen,E. (2005) Phylogenetic shadowing and computational identification of human microRNA genes. *Cell*, **120**, 21–24.
12. Bentwich,I., Avniel,A., Karov,Y., Aharonov,R., Gilad,S., Barad,O., Barzilai,A., Einat,P., Einav,U., Meiri,E. *et al.* (2005) Identification of hundreds of conserved and nonconserved human microRNAs. *Nature Genet.*, **37**, 766–770.
13. Lagos-Quintana,M., Rauhut,R., Yalcin,A., Meyer,J., Lendeckel,W. and Tuschl,T. (2002) Identification of tissue-specific microRNAs from mouse. *Curr. Biol.*, **12**, 735–739.
14. Ewing,B. and Green,P. (1998) Base-calling of automated sequencer traces using phred. II. Error probabilities. *Genome Res.*, **8**, 186–194.
15. Hofacker,I.L. (2003) Vienna RNA secondary structure server. *Nucleic Acids Res.*, **31**, 3429–3431.
16. Thompson,J.D., Higgins,D.G. and Gibson,T.J. (1994) CLUSTAL W: improving the sensitivity of progressive multiple sequence alignment through sequence weighting, position-specific gap penalties and weight matrix choice. *Nucleic Acids Res.*, **22**, 4673–4680.
17. Bonnet,E., Wuyts,J., Rouze,P. and Van de Peer,Y. (2004) Evidence that microRNA precursors, unlike other non-coding RNAs, have lower folding free energies than random sequences. *Bioinformatics*, **20**, 2911–2917.
18. Berezikov,E., van Tetering,G., Verheul,M., van de Belt,J., van Laake,L., Vos,J., Verloop,R., van de Wetering,M., Guryev,G., Takada,S. *et al.* (2006) Many novel mammalian microRNA candidates identified by extensive cloning and RAKE analysis. *Genome Res.*, in press.
19. Kloosterman,W.P., Wienholds,E., de Bruijn,E., Kauppinen,S. and Plasterk,R.H. (2006) *In situ* detection of miRNAs in animal embryos using LNA-modified oligonucleotide probes. *Nature Meth.*, **3**, 27–29.
20. Chenchik,A., Zhu,Y.Y., Diatchenko,L., Li,R., Hill,J. and Siebert,P.D. (1998) In Siebert,P.D. and Larrick,J. (eds.), *Gene Cloning and Analysis by RT–PCR*. BioTechniques Books, MA, pp. 305–319.
21. Ambros,V., Bartel,B., Bartel,D.P., Burge,C.B., Carrington,J.C., Chen,X., Dreyfuss,G., Eddy,S.R., Griffiths-Jones,S., Marshall,M. *et al.* (2003) A uniform system for microRNA annotation. *RNA*, **9**, 277–279.

22. Berezikov,E., Cuppen,E. and Plasterk,R.H. (2006) Approaches to microRNA discovery. *Nature Genet.*, **38**, S2–S7.
23. Barad,O., Meiri,E., Avniel,A., Aharonov,R., Barzilai,A., Bentwich,I., Einav,U., Gilad,S., Hurban,P., Karov,Y. *et al.* (2006) MicroRNA expression detected by oligonucleotide microarrays: system establishment and expression profiling in human tissues. *Genome Res.*, **14**, 2486–2494.
24. Mineno,J., Okamoto,S., Ando,T., Sato,M., Chono,H., Izu,H., Takayama,M., Asada,K., Mirochnitchenko,O., Inouye,M. *et al.* (2006) The expression profile of microRNAs in mouse embryos. *Nucleic Acids Res.*, **34**, 1765–1771.

Available online at www.sciencedirect.com
SCIENCE DIRECT®
ELSEVIER
Leukemia Research 30 (2006) 1105–1112
Leukemia Research
www.elsevier.com/locate/leukres

Expression of the myeloperoxidase gene in AC133 positive leukemia cells relates to the prognosis of acute myeloid leukemia

Jun Taguchi [a], Yasushi Miyazaki [a,*], Chizuko Tsutsumi [a], Yasushi Sawayama [a], Koji Ando [a], Hideki Tsushima [a], Takuya Fukushima [a], Tomoko Hata [a], Shinichiro Yoshida [b], Kazutaka Kuriyama [c], Sumihisa Honda [d], Itsuro Jinnai [a], Hiroyuki Mano [e], Masao Tomonaga [a]

[a] *Department of Hematology and Molecular Medicine Unit, Atomic Bomb Disease Institute, Nagasaki University Graduate School of Biomedical Sciences, 1-12-4 Sakamoto, Nagasaki 852-8523, Japan*
[b] *Department of Internal Medicine, Nagasaki National Medical Center, 2-1001-1 Ohmura, Nagasaki 856-8562, Japan*
[c] *School of Health Sciences, University of the Ryukyus, Nishihara, Okinawa 903-0215, Japan*
[d] *Department of Radiation Epidemiology, Atomic Bomb Disease Institute, Nagasaki University Graduate School of Biomedical Sciences, 1-12-4 Sakamoto, Nagasaki 852-8523, Japan*
[e] *Divisions of Functional Genomics, Jichi Medical School, 3311-1 Minamikawachi-machi Yakushiji, Kawachi-gun, Tochigi 329-0498, Japan*

Received 15 October 2005; received in revised form 30 December 2005; accepted 30 December 2005
Available online 2 February 2006

Abstract

We previously reported that the percentage of myeloperoxidase (MPO) positive blasts had a prognostic impact on survival of patients with acute myeloid leukemia (AML). To extend this observation, we quantitatively measured the level of the MPO gene in AC133 positive leukemia cells that would contain a putative AML stem/progenitor compartment. AML cases were divided into the MPO gene high (MPOg-H) and MPO gene low (MPOg-L) groups. Only patients belonging to the MPOg-H group had a favorable chromosomal translocation, t(8;21), and having no morphological dysplasia that was associated with MPOg-L. The difference in the survival of MPOg-H and MPOg-L was statistically meaningful, demonstrating the possible prognostic impact of the expression of MPO gene in AC133 positive leukemia cells.

Keywords: Myeloperoxidase; Gene expression; AC133; Acute myeloid leukemia; Prognostic factor

1. Introduction

Myeloperoxidase (MPO) is an enzyme exclusively expressed in hematopoietic cells committed to myeloid lineage [1–4]. Based on its specific expression in normal myeloid cells, both the enzymatic activity and the presence of MPO protein in leukemia blasts have been used for the diagnosis of acute myeloid leukemia (AML) by the French–American–British (FAB) group [5] as prime markers for the myeloid lineage of leukemia blasts.

Apart from its role in diagnosis, MPO in leukemia blasts was also shown to have a prognostic value by several groups [6–8]. In our recent report [8], AML patients with high percentage of MPO positive blasts (>50% of blasts are MPO activity positive, blast MPOa-H group) defined by routine cytochemical staining had a significantly better outcome compared to the low MPO activity positive blast group (MPO activity positive blasts ≤ 50%, blast MPOa-L). Multivariate analysis picked up the percentage of MPO positive blast as an independent prognostic factor along with karyotypes, WBC count at diagnosis and age. Considering that most of AML cases with favorable karyotyes, such as t(8;21) or inv(16) belong to the blast MPOa-H group (83 out of 88 cases in our previous report), it is suggested that MPO is one of the proteins highly expressed in leukemia blasts of AML cases with favorable prognosis by conventional chemotherapy.

Abbreviations: AML, acute myeloid leukemia; FAB, French–American–British; GAPDH, glyceraldehyde-3-phosphate dehydrogenase; MLD, multilineage myelodysplasia; MPO, myeloperoxidase; PBS, phosphate-buffered saline; WBC, White blood cell

* Corresponding author. Tel.: +81 95 849 7111; fax: +81 95 849 7113.
E-mail address: y-miyaza@net.nagasaki-u.ac.jp (Y. Miyazaki).

0145-2126/$ – see front matter © 2006 Elsevier Ltd. All rights reserved.
doi:10.1016/j.leukres.2005.12.012

Recent studies on leukemia cell populations revealed that a hierarchy of differentiation exists in AML blasts consisting of leukemia stem/progenitor cells and maturing blast cells. AML stem cells that are transplantable into NOD-SCID mice constitute a small proportion of leukemia cell population and they bear surface markers usually found on normal hematopoietic stem cells, such as CD34 and AC133 (CD133, PROMININ1 [PROM1]) [9–14]. CD133 expression has been demonstrated not only on hematopoietic stem cells shown by the reconstitution of hemtopoiesis using transplantation model but also on other tissue cells, such as undifferentiated epithelium and fetal brain neural stem cells. It is suggested that CD133 could be expressed on the surface of various stem/progenitor cells [15]. These antigens were successfully used to select leukemia stem cells to analyze, for example, the gene expression profile in hematopoietic stem cells or leukemia stem cells [9,14–17]. We have also examined the expression of more than 12,000 genes in AC133 positive leukemia cells, and compared the gene expression profiles between AML cases with and without morphological dysplasia (AML with multilineage dysplasia, AML/MLD and AML/non-MLD), demonstrating the different gene expression profiles in these two groups [18]. In this analysis, we also found that, in AC133 positive AML cells, MPO gene was expressed more in cases without dysplasia than those accompanied with dysplasia (Tsutsumi et al., unpublished data). Since AML/MLD tends to have a worse prognosis than AML/non-MLD [19], the expression of the MPO gene in AC133 positive cells seemed in accordance with the relationship between clinical outcome of AML and the percentage of MPO positive blasts judged by cytochemichal examination of bone marrow smears. These results suggested that the MPO gene would be expressed in an immature fraction of leukemia cells that contains leukemia stem cells, and that the expression level of the MPO gene in AC133 positive cells might be also related to prognosis.

With these backgrounds, we quantitatively measured the expression of the MPO gene in AC133 positive leukemia cells and we found that the level of MPO gene expression divided AML cases into two groups: MPO gene high (MPOg-H) and MPO gene low (MPOg-L).

We confirmed that all AML/MLD cases belonged to MPOg-L. We could also demonstrate the prognosis of MPOg-H group was better than MPOg-L, and that karyotypes related to poor prognosis were found only in MPOg-L. These findings suggested that the level of MPO gene expression in AC133 leukemia cells related to the prognosis of AML.

2. Materials and methods

2.1. Cell separation and purification

After obtaining written informed consent, bone marrow samples were collected from 33 patients with de novo AML before treatment and from 10 healthy volunteers as control.

Table 1
Percentage of AC133 positive cells before and after purification

Case number	Before purification (%)	After purification (%)
7	14	97.4
8	74.5	99.6
9	12.1	98.8
11	63	84.3
14	36.2	99.3
16	65.4	98.8
17	72.4	94.1

The method to purify AC133 positive cells was described previously [18]. Shortly, target cells were selected from bone marrow mononuclear cells with anti-AC133 antibody-conjugated magnetic microbeads and MACS magnetic separation columns (AC133 Isolation Kit, Miltenyi Biotec, Bergisch-Gladbach, Germany).

When the number of AC133 positive cells was more than 1×10^6 after selection (seven cases, Table 1), the percentage of AC133 positive cells was assessed before and after purification using a flowcytometer (FACScan, Becton Dickinson, Oxford, UK) and anti-AC133/2 antibody (Miltenyi Biotec). In other cases, the isolated cells were morphologically examined on cytospin slides (May–Grunwald–Giemsa staining) to check the contamination of promyelocytes.

2.2. Quantitative real-time PCR (RT-PCR)

The expression of the MPO gene was assessed using quantitative real-time PCR method. cDNA was synthesized from total cellular RNA isolated from purified AC133 positive cells (using RNeasy mini, QIAGEN GmbH, Hilden, Germany) with oligo dT primer (ProSTARTM First-strand cDNA Kit, STRATAGENE, CA, USA), that was used as a template for the PCR reaction. RT-PCR was performed using LightCycler, SYBR Green System (Roche Diagnostics, Basel, Switzerland) following the manufacturer's instructions. The PCR was conducted for 40 cycles (95 °C for 15 s, 60 °C for 10 s and 72 °C for 7 s as one cycle) and 45 cycles to amplify the MPO gene and the GAPDH gene, respectively. The sequences of the PCR primer sets were as follows: for MPO gene, 5′-AACTGATGGAGCAGTATGGCACGC-3′ and 5′-TCGCTGCTGCATGCTGAACACACC-3′ and for the GAPDH gene, 5′-GTCAGTGGTGGACCTGACCT-3′ and 5′-TGAGCTTGACAAAGTGGTCG-3′. Data of RT-PCR were standardized with the following control samples: cDNA of the U937 cell line for GAPDH (quantitative range, 10^0 to 10^{-6}) and MPO cDNA for MPO (quantitative range, 10^0 to 10^{-6}). In cases with chromosomal translocation between 8 and 21, AML1-ETO fusion transcript was also quantitatively assessed before and after the purification of AC133 positive fraction (primer sets for the AML1-ETO fusion gene, 5′-CACCTACCACAGAGCCATCAAA-3′ and 5′-ATCCACAGGTGAGTCTGGCATT-3′) [20]. All PCR reactions were performed at least twice. The amplification of target genes were confirmed by examining the melting

curves of products and by the electrophoresis of PCR products on a 2% agarose gel followed by the visualization with ethidium bromide staining.

2.3. Cell staining

In some cases, to show the presence of MPO protein and its enzymatic activity, AC133 positive cells spread on the slides were stained with anti-MPO antibody (Nichirei Corporation, Tokyo, Japan) using a DAKO LSAB + Kit (DAKO Corporation, CA, USA) and with the diaminobdnzidine method [21], respectively. The expression of MPO protein or its enzymatic activity was shown as a percentage of MPO (protein or activity) positive cells.

2.4. Cytogenetic risk group

Based on the karyotype of leukemia cells, patients were classified into either the favorable, intermediate or adverse risk group, defined by the MRC group with minor modification [22,23].

2.5. Statistical analyses

Clinical and hematological data were obtained from the medical record of each case. The comparison of multilineage dysplasia of hematopoietic cells in the presence of leukemia blasts [23] and the presence of Auer body between groups were analyzed using Chi-square test. The cytogenetic risk group was compared using Mantel extension test. WBC count and the percentage of MPO positive blasts among the groups were analyzed using Wilcoxon's rank sum test.

3. Results

3.1. Purification of AC133 positive cells

The percentage of AC133 positive leukemia cells in bone marrow varied from case to case (0.3–76.6% of mononuclear cells in 20 cases tested), and it did not have any relationship to the FAB subtypes of AML (data not shown) as reported previously [24,25]. After purification, an analysis with flowcytometer demonstrated that AC133 was positive in 84.4–99.6% of collected cells (median 98.8%) among seven cases in which we could obtained more than 1×10^6 cells (Table 1). Though the percentages of AC133 positive cells somewhat varied after purification, there was no differentiated myeloid cells, such as promyelocytes, under morphological evaluation of the slides.

Since some of normal stem cells have been shown to have AC133 antigen on its surface, we next assessed whether leukemia cells but not residual normal stem cells were selected by the purification procedure. For this purpose, we utilized cases with a specific chromosomal translocation, t(8;21), and the expression of AML1-ETO fusion gene resulting from this translocation was quantitatively measured after the purification. As shown in Table 2, the expression of AML1-ETO fusion gene was detected in all four cases though its level was distributed from 0.7 to 22.1. It demonstrated that the purified samples contained target leukemia cells in these four cases.

Table 2
Amount of AML1-ETO transcript after selection with AC133 columun

Case number	AML1-ETO/GAPDH ratio
3	7.77
4	22.1
10	0.7
11	4.88
Negative control[a]	<0.01
Kasumi-1 cell line[b]	167.02

[a] M1 case with normal karyptype.
[b] No selection procedure.

3.2. Quantitative measurement of the MPO gene by real-time RT-PCR method

The relative amount of MPO transcript was shown as a ratio of the MPO and GAPDH transcripts (MPO/GAPDH ratio), and the data are summarized in Table 3. Among control samples, the MPO/GAPDH ratio ranged from 3.2 to 11.8, showing similar values. On the other hand, the MPO/GAPDH ratios varied widely in AML cases (0.05–49.9). Referring to the distribution of the ratios among AML samples and that of normal control (Table 3), we divided the AML cases into two groups: MPO gene high group (MPO/GAPDH ratio > 15, MPOg-H, 10 cases) and MPO gene low group (MPO/GAPDH ratio $\leqq$ 15, MPOg-L, 23 cases) so that all normal controls belonged to the MPOg-L group (Fig. 1). In some cases, MPO protein and its enzymatic activity were also examined on the cytospin slides of AC133 positive cells (Table 4). The enzymatic activity of MPO in AC133 positive

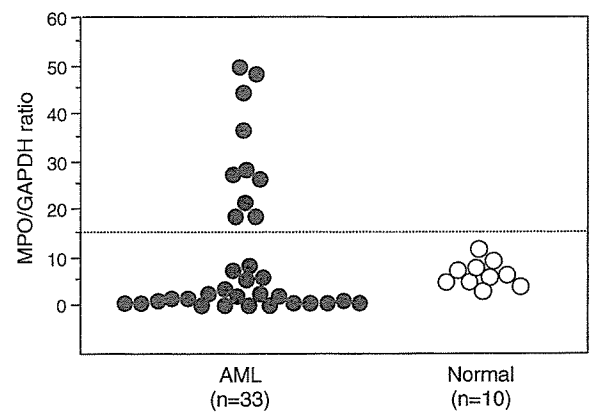

Fig. 1. Relative amount of MPO transcripts in AML cells (33 cases) and normal bone marrow cells (10 cases) selected with AC133-columns. The ratios of the MPO and GAPDH genes are shown as MPO/GAPDH ratio. AML cases were divided into two groups by the ratio (>15 and $\leqq$15). The dotted line shows the ratio, 15.

Table 3
MPO/GAPDH ratio and the percentage of MPO positive blasts

Case number	MPO/GAPDH ratio	BM blast-MPO	FAB	MLD	Cytogenetic risk group	MPOg group
1	7.37	50	M2	+	Adverse, 5q−	L
2	5.37	33	M6	+	Adverse, −5	L
3	44.26	100	M2	−	Favorable, t(8;21)	H
4	36.58	96	M1	−	Favorable, t(8;21)	H
5	0.65	6	M2	+	Adverse, complex	L
6	1.80	45	M2	+	Intermediate, normal	L
7	2.83	35	M2	+	Intermediate, normal	L
8	0.05	2	M0	−	Intermediate, others	L
9	0.07	10	M2	−	Intermediate, normal	L
10	21.46	100	M2	−	Favorable, t(8;21)	H
11	18.77	100	M2	−	Favorable, t(8;21)	H
12	2.35	13	M4	+	Adverse, complex	L
13	0.12	4	M4	−	Intermediate, others	L
14	0.60	3	M6	−	Adverse, complex	L
15	49.91	80	M1	−	Intermediate, normal	H
16	18.67	100	M4	−	Intermediate, others	H
17	8.50	80	M4-Eo	−	Favorable, inv(16)	L
18	0.92	60	M4	+	Intermediate, others	L
19	48.52	98	M2	−	Intermediate, others	H
20	27.55	99	M1	−	Intermediate, normal	H
21	28.34	94	M2	−	Intermediate, others	H
22	2.09	26	M2	+	Intermediate, normal	L
23	0.83	10	M4	−	Intermediate, normal	L
24	2.43	59	M2	+	Adverse, −5	L
25	1.33	2	M0	−	Intermediate, normal	L
26	3.78	80	M2	+	Intermediate, normal	L
27	0.09	5	M4	+	Intermediate, normal	L
28	26.48	100	M1	−	Intermediate, normal	H
29	0.66	84	M2	−	Intermediate, normal	L
30	1.11	45	M2	+	Adverse, complex	L
31	0.53	11	M2	+	Intermediate, normal	L
32	1.58	54	M4	+	ND	L
33	5.95	82	M2	+	Intermediate, normal	L
Normal 1	11.8	ND				
Normal 2	9.5	ND				
Normal 3	8.0	ND				
Normal 4	7.5	ND				
Normal 5	6.5	ND				
Normal 6	6.2	ND				
Normal 7	5.2	ND				
Normal 8	5.0	ND				
Normal 9	4.1	ND				
Normal 10	3.2	ND				

ND, not done; MLD, multilineage dysplasia.

cells was detected mostly in cases belonging to MPOg-H group, and they had high percentages of MPO protein positive cells except for case 33 (Table 4).

We next compared the level of expression of the MPO gene in AC133 positive cells and the percentage of MPO positive leukemia blasts judged on bone marrow slides. The relationship of these two factors is shown in Fig. 2. Cases were classified into the high percentage of MPO (activity) positive blasts (blast MPOa-H group, MPO activity positive blasts > 50%) or the low group (blast MPOa-L group, MPO activity positive blasts ≦ 50%). All cases in the blast MPOa-L group were categorized into MPOg-L (Group III), however, the blast MPOa-H cases comprised of MPOg-H (Group I, 10 cases) and MPOg-L (Group II, 8 cases). It meant that cases in Group II showed high percentage of MPO positive blast on the bone marrow smear but the expression of the MPO gene was low in the AC133 positive fraction. The percentage of MPO positive blasts did not have a statistically significant prognostic impact on overall survival in this series (Fig. 3) but all long-term survivors belonged to the MPOg-H group.

3.3. Clinical characteristics of cases in MPOg-H and MPOg-L groups

Clinical characteristics of AML cases in the MPOg-H and MPOg-L groups are shown in Table 5. There was no statistical difference in age or performance status (PS) among these two groups, however, multilineage morphological dysplasia

Table 4
Percentages of MPO protein or MPO activity positive cells among AC133 purified samples

Case number	MPO/GAPDH ratio	MPOg group	AC133-MPO protein positive cell (%)	AC133-MPO activity positive cell (%)
13	0.12	L	0	0
14	0.60	L	<1	0
17	8.50	L	13	0
18	0.92	L	10	0
19	48.52	H	100	12
20	27.55	H	100	60
21	28.34	H	100	29
23	0.83	L	0	0
24	2.43	L	3	0
25	1.33	L	0	0
26	3.78	L	11	0
28	26.48	H	100	64
31	0.53	L	0	0
32	1.58	L	0	0
33	5.95	L	47	5

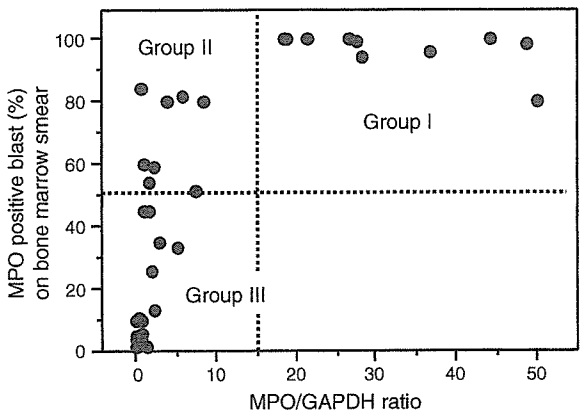

Fig. 2. Relationship between the percentage of MPO positive blasts on bone marrow smear and the amount of the MPO gene in AC133 positive cells. AML cases were categorized into three groups (Groups I–III) by the two factors above. The vertical dotted line shows the MPO/GAPDH ratio, 15, and the horizontal one is for the percentage of MPO positive blasts, 50%. There were 10 cases in Group I, 8 cases in Group II and 15 cases in Group III.

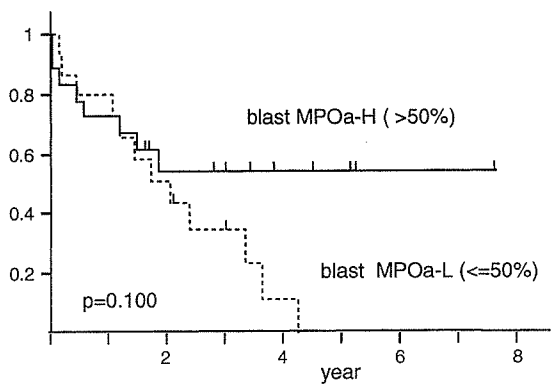

Fig. 3. Overall survival by the percentage of MPO positive blasts on bone marrow smear. There was no statistical significance between the high MPO group (blast MPOa-H) and the low MPO group (blast MPOa-L). The p-value was 0.100.

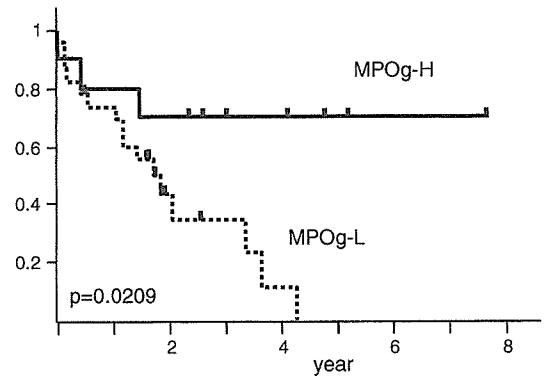

Fig. 4. Overall survival by the amount of MPO gene expression in AC133 positive cells. AML cases with high expression of the MPO gene in AC133 positive cells (MPOg-H) showed better overall survival than those with low expression (MPOg-L) with statistical significance ($p = 0.0209$).

(MLD) in the presence of leukemia blasts was found only in the cases belonging to the MPOg-L group. Distribution of cases in the chromosomal risk groups was also significantly different between MPOg-H and MPOg-L; four out of five cases with favorable karyotypes were in the MPOg-H, and all seven cases with adverse chromosomal risk belonged to the MPOg-L group. Interestingly, although the WBC count at diagnosis was significantly high in the MPOg-H group, overall survival was better in the MPOg-H group than the MPOg-L with statistical significance (Fig. 4).

4. Discussion

Recent reports have demonstrated that AC133 positive bone marrow/cord blood cells are capable of reconstituting long-term hematopoiesis both in mouse and man [12,13,26,27], and that human AML blasts bearing AC133 are able to proliferate and form a leukemic cell population in NOD-SCID mice [11]. From these reports, it has been suggested that normal and malignant hematopoietic stem cells